Supplementary Information for: Large-area, high-numerical-aperture, freeform Metasurfaces

You Zhou[1†], Chenkai Mao[1†], Erez Gershnabel[1,2], Mingkun Chen[1], and Jonathan Fan[1*]

[1]Department of Electrical Engineering, Stanford University, Stanford, California, 94305, USA
[2]Israel Aerospace Industries, Ben Gurion International Airport, Lod 7010000, Israel

†Authors contributed equally
*email: jonfan@stanford.edu

Section 1: Reparameterization formalism

We consider a super-pixel with wavelength-scale dimensions L_x and L_y, which is divided into N subcells along *x*-axis direction. Within the *m*th subcell there is an elliptically-shaped nanopost element with a defined length (a_m), width (b_m) and position ($\Delta x_m, \Delta y_m$) (Fig. S1).

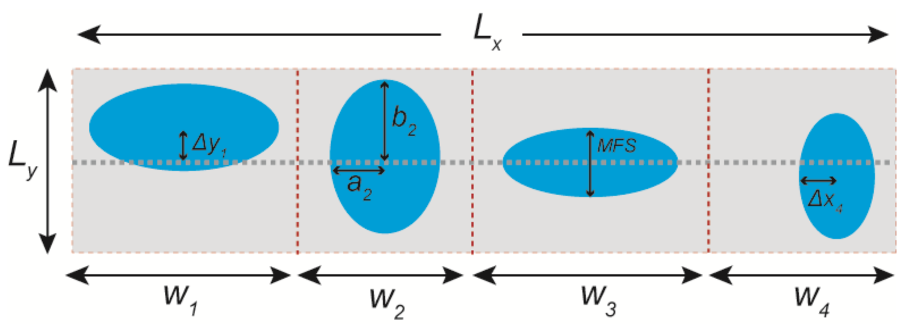

Fig. S1| Schematic of a freeform metasurface device. Schematic of a super-pixel with wavelength-scale dimensions L_x and L_y. The super-pixel is divided into multiple subcells along *x*-axis direction. Each subcell consists of a nonrotated elliptical nanopost described by a defined length (a_m), width (b_m) and position ($\Delta x_m, \Delta y_m$)

We apply user-defined minimum feature size (MFS) to ensure that the dimensions of ellipses align with the fabrication capabilities. The geometric parameters of the elliptically-shaped nanoposts are represented by unconstrained and continuous latent variables, which are described by a $1 \times (N-1)$ vector, using differentiable analytical functions. The width of each subcell w_m satisfy the following constraints:

$$\sum_{m=1}^{m=N} w_m = L_x$$

$$w_m \geq w_{min} \tag{1}$$

w_{min} defines the minimum subcell dimension with values greater than $2MFS$. The following expressions describe the width of each subcell based on the formalism[1,2]

$$s_i = \frac{e^{u_i}}{e^{u_i} + 1}, s_N = 1, i = 1, \dots, N-1$$

$$t_1 = s_1$$

$$t_1 = s_i \sqrt{1 - \sum_{j=1}^{i-1} t_j^2}, i = 2, \dots, N$$

$$w_m = \frac{t_m}{\sum_{j=1}^{N} j}(L_x - Nw_{min}) + w_{min}, m = 1, \dots, N \tag{2}$$

The latent variables within each subcell are described by a two-dimensional tensor (v_{mx}, v_{my}), where v_{mx} and v_{my} represent the variables that parametrizes the width and length of the *m*th subcell, respectively. For each subcell, the analytical transformation is obtained to transform the latent variables to the ellipse dimensions:

$$a_m = \left[(w_m - MFS/2) - \frac{MFS}{2}\right]\frac{e^{v_{mx}}}{e^{v_{mx}} + 1} + MFS/2$$

$$b_m = \left[\left(L_y - MFS/2\right) - \frac{MFS}{2}\right]\frac{e^{v_{my}}}{e^{v_{my}+1}} + MFS/2 \tag{3}$$

The normalized permittivity profile within the *m*th subcell can be defined

$$\varepsilon_m(x_m, y_m, a_m, b_m, T_1) = \exp\left(-\left(\frac{x_m^2}{a_m^2} + \frac{y_m^2}{b_m^2}\right)^{1/T_1}\right)$$

$$x \in [-w_m/2, w_m/2], y \in [-L_y/2, L_y/2] \tag{4}$$

where x_m, y_m define the center of ellipse in the mth subcell. T_1 is a hyperparameter used in adiabatic toggling to transform permittivity distribution from grayscale to binary values. During each optimization, T_1 is dynamically adjusted from high to low values. At the beginning, a higher value of T_1 allows for larger modifications to the device layout. As the optimization advances, T_1 is reduced to ensure a more accurate representation of the binary physical device. The gradients of Figure of Merit (FOM) with respect to permittivity distribution are calculated with the adjoint variables method[3]. The use of backpropagation via the chain rule gives the gradients of the FOM with respect to the latent variables.

Section 2: Reparameterized adjoint variables method compared to conventional approach

To benchmark the performance between our reparameterized adjoint variables method and conventional approach, we design a wavelength-scale super-pixel that can deflect light into -50° angle at the wavelength of 900 nm. The super-pixel is 3λ-wide with minimum feature and gap sizes of 100 nm. Fig. S3a shows the top view of a super-pixel designed using reparameterized adjoint variables method. The polar plot of farfield scattering (Fig. S3b) demonstrates strong scattering in the desired direction with 78% efficiency. As a control example, we design a super-pixel with the same defection angle using conventional phase arrays (Fig. S3c). The polar plot of farfield scattering (Fig. S3d) reveals reduced efficiency (50%) and significant undesired scattering.

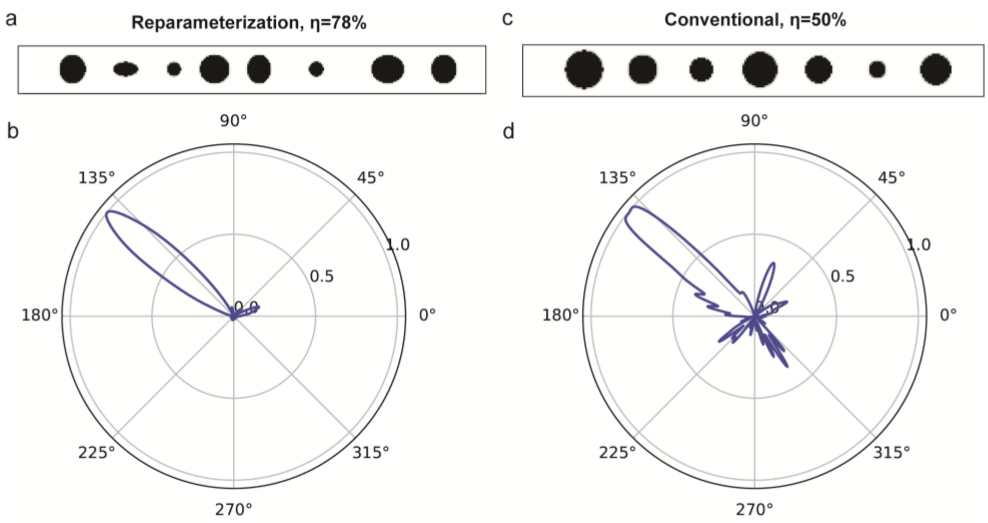

Fig. S3| (a) Top view of a super-pixel designed using reparameterized adjoint variables method. The super-pixel is designed to deflect light at -50° angle with 78% efficiency. (b) Polar plot of farfield scattering. (c-d) The same deflector designed based on conventional phase arrays, showing significant undesired scattering and reduced efficiency (50%).

Section 3: High-NA wavelength multiplexing metalens

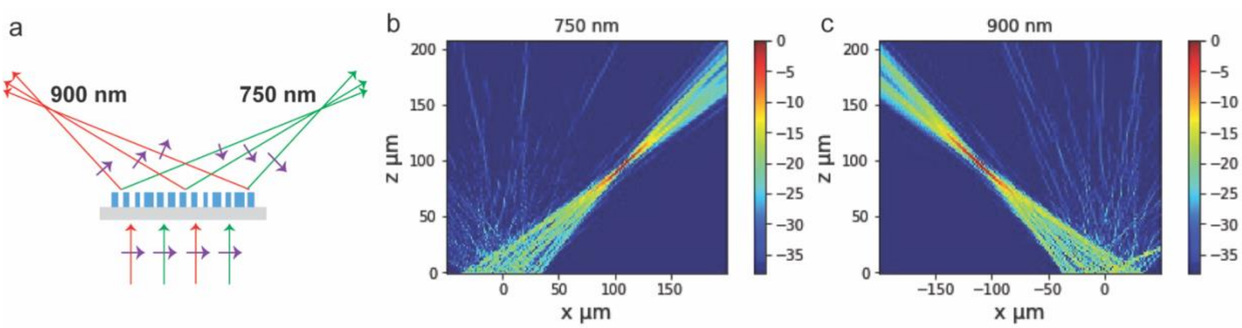

Fig. S3| (a) A schematic of a wavelength multiplexed metalens designed to focus light at extremely large off-axis positions, with independently specified focusing displacements for 750 nm and 900 nm. The device is 74- µm wide and focuses transverse magnetic (TM) polarized light to horizontal positions of -111 µm and 110 µm for 750 nm and 900 nm, respectively. (b-c) Full-wave simulations of the axial intensity distributions for 750 nm (b) and 900 nm (c).

Section 4: Simulated results for metadevice generating donut-shaped point spread functions

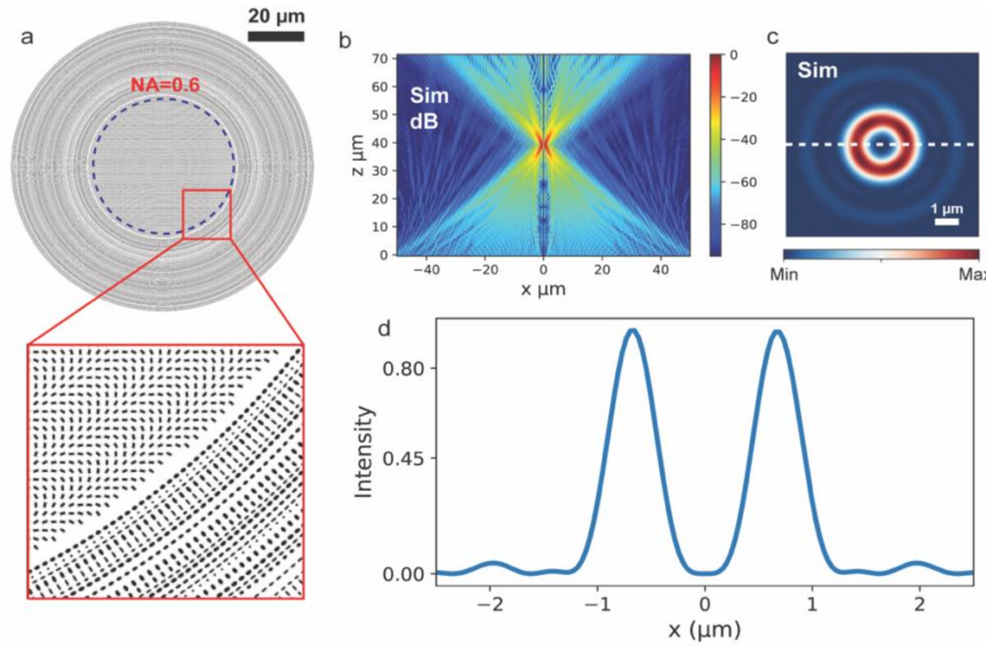

Fig. S4 Metadevices for generation and focusing of vortex beams. (a) Top view of a metadevice for high numerical aperture (NA=0.8) focusing of vortex beams with a topological charge of $m = 2$. The low numerical aperture (NA<=0.6) section is designed using conventional half-wave plate elements, while the high numerical aperture (NA>0.6) section is filled with radially patterned aperiodic deflectors. (b) Full-wave simulations of the axial intensity distribution. (c) Point spread function (PSF) at the focal plane. (d) One-dimensional horizontal cut of PSF along the whited dashed line denoted in c.

References

1. Chen, M., Jiang, J. & Fan, J. A. Design Space Reparameterization Enforces Hard Geometric Constraints in Inverse-Designed Nanophotonic Devices. *ACS Photonics* **7**, 3141–3151 (2020).
2. Gershnabel, E. *et al.* Reparameterization Approach to Gradient-Based Inverse Design of Three-Dimensional Nanophotonic Devices. *ACS Photonics* (2022). doi:10.1021/acsphotonics.2c01160
3. Lalau-Keraly, C. M., Bhargava, S., Miller, O. D. & Yablonovitch, E. Adjoint shape optimization applied to electromagnetic design. *Opt. Express* **21**, 21693 (2013).